Journal of Fluorine Chemistry 217 (2019) 90–96

Contents lists available at ScienceDirect

Journal of Fluorine Chemistry

journal homepage: www.elsevier.com/locate/fluor

Thermodynamic description for the NaF-KF-RbF-ZnF_2 system

Huiqin Yin, Shuang Wu, Xueliang Wang, Long Yan, Wenguan Liu*, Zhongfeng Tang*

Shanghai Institute of Applied Physics, Chinese Academy of Sciences, Shanghai, 201800, China

ARTICLE INFO

Keywords:
Molten fluoride salt
NaF-KF-RbF-ZnF_2
Calphad
Thermodynamic calculation

ABSTRACT

Thermodynamic evaluations and optimizations of the NaF-ZnF_2, KF-ZnF_2, RbF-ZnF_2, NaF-RbF and KF-RbF systems were determined by use of the CAlculation of PHAse Diagrams (CALPHAD) approach in this work. The subregular solution model was applied to model liquid phase, while the stoichiometric compound model was used to describe the intermediate phases. All the model parameters were evaluated on the basis of the required thermochemical and phase equilibrium data from experimental measurements in literature and theoretical predictions from first-principles method. A set of self-consis5tent and reliable thermodynamic database for the NaF-KF-RbF-ZnF_2 quaternary system was finally derived by merging the model parameters of relevant binary systems (model parameters of NaF-KF were adopted from the literature) based upon the Muggianu extrapolation model. The invariant reactions of ternary systems from NaF-KF-RbF-ZnF_2 were obtained according to the database. This work will provide beneficial instructions in the relevant multi-components molten salt design in industrial fields.

1. Introduction

Molten fluoride salts, which is thermal stable, resembles water at room temperature being optically transparent and has the similar heat capacity, about the three times viscosity, roughly twice density at 700 °C [1–3], have been considered and/ or proposed as heat transfer media for Molten Salt Reactor [4], Next Generation Nuclear Plant to the Nuclear Hydrogen Initiative heat transfer loop [5], Concentrating Solar Power [6], electro-winning [7] and so on. However, fluoride salt can freeze and block the heat transfer loop in the evening or on cloudy days, because of their high melting temperature [8]. Therefore, it is significant and indispensable to develop fluoride salt with a low melting temperature by their thermodynamic phase equilibrium information. Multicomponent salt generally tends to lower the melting temperature, and the eutectic composition has the lowest melting point in the system.

The quaternary NaF-KF-RbF-ZnF_2 system was studied in the present work, where NaF, KF are the most common candidate molten salt with generally low cost, and the rest have relative low melting point. The experimental phase equilibria information on the NaF-KF system has been investigated by several researchers [9–15]. The results showed that the NaF-KF is a simple eutectic system, and the eutectic point appears at about 972–994 K & 40 mol% NaF. This system has been extensively described by Wang [16] in 2013. The optimized parameters of NaF-KF are directly used without further elaborations here. Only two groups of researchers have reported the phase equilibria information on the NaF-ZnF_2 system [17,18]. An intermediate phase $NaZnF_3$ was discovered and congruently melted in this system. Two eutectic reactions with end-member (NaF and ZnF_2, respectively) were formed on both sides of $NaZnF_3$. However, there exist small discrepancies about the reported congruent temperature of $NaZnF_3$ and two eutectic temperatures Kozak observed that $NaZnF_3$ could be congruently melted at 1028.15 K, which is 7 K higher than the temperature measured by Barton [17]. A larger controversy is the two eutectic point positions. The former observed that the two eutectic points were placed at 0.66 mol ZnF_2 & 983.15 K and 0.330 mol ZnF_2 & 925.15 K, compared with 0.690 mol ZnF_2 & 958.15 K and 0.330 mol ZnF_2 & 908.15 K by the latter, respectively. The complete phase diagram of KF-ZnF_2 and RbF-ZnF_2 systems have only been studied by Barton at Oak Ridge National Laboratory in 1952 [17], which were unpublished work and compiled in ORNL report No.2548. Equilibrium phase relation for the KF-ZnF_2 is very similar to NaF-ZnF_2 system. The former contains two intermediate phases K_2ZnF_4 and $KZnF_3$ (they could be incongruently and congruently melted at 993.15 K and 1123.15 K, respectively), compared with two intermediate phases Rb_2ZnF_4 and $RbZnF_3$ by the latter (they incongruently and congruently melted at 893.15 K and 1003.15 K, respectively). For NaF-RbF binary system, mainly two research groups [12,17] have determined the experimental phase equilibrium measurements. Both of them proved that NaF-RbF is a simple eutectic system, but

* Corresponding authors. Present address: Shanghai Institute of Applied Physics, Chinese Academy of Sciences, Jialuo Road 2019, Jiading District, Shanghai, 201800, China.

E-mail addresses: liuwenguan@sinap.ac.cn (W. Liu), tangzhongfeng@sinap.ac.cn (Z. Tang).

https://doi.org/10.1016/j.jfluchem.2018.09.008
Received 9 August 2018; Received in revised form 18 September 2018; Accepted 25 September 2018
Available online 27 September 2018

discrepancies still exist on the eutectic position. Holm [12] reported that the eutectic position is located at 940.15 K & 0.672 mol RbF, compared with 948.15 ± 10 K & 0.730 mol RbF observed by Barton [17]. Equilibrium phase relation for KF-RbF has mainly been conducted by two groups of researchers [17,19]. Both studies reported that KF-RbF is an isomorphous system with a minimum at 1043.15 K & 0.72 mol RbF. However, there are only liquidus experimental data of KF-RbF, and no related data defining the solidus line.

Although there are some experimental investigations on the preceding binary systems in the NaF-KF-RbF-ZnF_2, thermodynamic evaluation for the NaF-KF-RbF-ZnF_2 system and corresponding database are still not reported until now, which are of most importance for preparing and screening molten salt with superior properties, studying the ionic interactions and evaluating the service behavior in this system. What's more, it is difficult to obtain them based on the experiments alone, due to the experiment measurements difficulty and lots of uncertainty at relative high temperature. CAlculation of PHAse Diagrams (CALPHAD) [20,21] is considered to be an effective and viable approach in calculating phase diagram and thermodynamic properties of the multi-components molten salts. This method has been successful for optimizing a large amount of molten salt systems (such as nitrate molten salt [22,23], chloride molten salt [24], fluoride molten salt [25–27] and so on), and employed to compute and predict the low-melting points compositions in this system.

In the present work, all the binary systems of quaternary NaF-KF-RbF-ZnF_2, except the NaF-KF system, were thermodynamically modeled using the subregular solution model based on the phase equilibrium data in literature and theoretical data predicted from the first-principles approach. A set of self-consistent and reliable thermodynamic database for the NaF-KF-RbF-ZnF_2 quaternary system was finally derived by merging the model parameters of relevant binary systems (model parameters of NaF-KF were adopted from the literature) based upon the Muggianu extrapolation model. The invariant reactions of all the ternary systems and minimum liquidus points concerning NaF-KF-RbF-ZnF_2 quaternary system were predicted according to the database. Thermodynamic properties and phase equilibrium concerning NaF-KF-RbF-ZnF_2 system could be calculated by use of the present developed thermodynamic database. This work will provide beneficial instructions in the relevant multi-components molten salt design in industrial fields.

2. Methodologies of thermodynamic calculation

2.1. First-principles calculation

When lacking of relative experiment measurements for some systems, theoretical predictions from first-principles calculation [28] can be used to supplement thermodynamic modeling, in order to reduce uncertainties of optimized parameters.

The thermochemical information is unavailable on the intermediate phases $NaZnF_3$, $RbZnF_3$, K_2ZnF_4 and $KZnF_3$. First-principles calculation was applied to predict their formation enthalpies. The total energies of the intermediate phases were calculated by Vienna ab-initio simulation package (VASP) [29]. Generalized gradient approximation (GGA) [30] was employed to describe the exchange correlation energy. Projector Augmented Wave (PAW) method [31] was used to describe electron-ion interactions. Plane-wave basis set was used to expand the wave functions with a cutoff energy of 500 eV. The positions of atoms were relaxed with tolerances of 0.01 eV/Å for the forces on each ion and with the convergence energy of 10^{-6} eV.

Then, their formation enthalpies with reference to NaF, KF, RbF and ZnF_2 can be obtained by the following Eqs. (1)–(4).

$$\Delta_f H_{NaZnF_3} = E_{tot}(NaZnF_3) - E_{tot}(NaF) - E_{tot}(ZnF_2) \quad (1)$$

Table 1
Single point energy of intermediate phases of the MF-ZnF_2 (M = Na, K and Rb) system from first-principles calculation (*: This work).

Compound	Space group	Single point energy	resource
NaF	$Fm\bar{3}m$	−8.754 eV	[25]
KF	$Fm\bar{3}m$	−27.431 eV	[26]
RbF	$Pm\bar{3}m$	−7.956 eV	[*]
ZnF_2	$P4_2/mnm$	−11.954 eV	[*]
$NaZnF_3$	$Pbnm$	−20.854 eV	[*]
$RbZnF_3$	$P6_3/mnc$	−20.553 eV	[*]
$KZnF_3$	$Pm\bar{3}m$	−20.678 eV	[*]
KF	$Pm\bar{3}m$	−6.612 eV	[26]
RbF	$Fm\bar{3}m$	−8.174 eV	[*]
RbF	$Pm\bar{3}m$	−7.960 eV	[*]
ZnF_2	$Pbcn$	−11.938 eV	[*]
$NaZnF_3$	$Pnma$	−20.855 eV	[*]
K_2ZnF_4	$I4/mmm$	−29.090 eV	[*]

$$\Delta_f H_{RbZnF_3} = E_{tot}(RbZnF_3) - E_{tot}(RbF) - E_{tot}(ZnF_2) \quad (2)$$

$$\Delta_f H_{K_2ZnF_4} = E_{tot}(K_2ZnF_4) - 2 \times E_{tot}(KF) - E_{tot}(ZnF_2) \quad (3)$$

$$\Delta_f H_{KZnF_3} = E_{tot}(KZnF_3) - E_{tot}(KF) - E_{tot}(ZnF_2) \quad (4)$$

where E_{tot} is the single point energy of corresponding component at 0 K listed in Table 1. Actually, KF and RbF have more than one allotropic form, and the more stable form $Fm\bar{3}m$ for KF, $Fm\bar{3}m$ for RbF and $P4_2/mnm$ for ZnF_2 were chosen to calculate their formation enthalpy. Herein, the cell parameters of intermediate phases are cited from Inorganic Crystal Structure Database (ICSD). However, first-principles calculation failed to calculate the formation enthalpy of Rb_2ZnF_4, due to the lack of relevant information on the crystal structure and lattice parameters.

2.2. Prediction for component concentrations in melts

There are no experimental data for the ternary systems of NaF-KF-RbF-ZnF_2. It is necessary to predict their properties, as only through brute force experimental measurements is not feasible. A method to predict the component concentrations was applied here, which was proposed by Martynova and Susarev [32] and based on the triangular Gibbs diagrams to compute the ternary eutectic concentrations. The relevant equations [33] are shown as follows.

$$D_A^{A,B} = \frac{2.3}{x_B^{A,B}} \ln\left(\frac{T_A x_A^{A,B}}{T_{fus}^{A,B}}\right) \quad (5)$$

$$P(A) = |(D_B^{A,B} - D_C^{A,C})(D_B^{B,C} - D_C^{B,C})| \quad (6)$$

where $x_B^{A,B}$ and $x_A^{A,B}$ are the eutectic concentration of component B and A in the binary A-B binary system, T_A and $T_{fus}^{A,B}$ is the melting point of components A and eutectic temperature of the A-B system. $D_A^{A,B}$ and $P(A)$ are the derivatives and stability applied from reference [34]. $D_C^{A,C}$, $D_B^{B,C}$ and $D_C^{B,C}$ are calculated from Eq. (5).

Herein, $P(A) \geq 0.15$ the following set of equations was used to predict the component concentration in this work.

$$\Delta x_A^{A,B,C} = (T_A - T_{fus}^{B,C})\left(\frac{\Delta x_A^{A,B} x_B^{B,C}}{T_A - T_B} + \frac{\Delta x_A^{A,C} x_C^{B,C}}{T_A - T_C}\right) \quad (7)$$

$$\Delta x_A^{A,B} = |0.5 - x_A^{A,B}| \quad (8)$$

and

$$\Delta x_A^{A,C} = |0.5 - x_A^{A,C}| \quad (9)$$

Table 2
Phase and crystal structure and thermodynamic model used in this work.

Phase name	Space group	Model	Model description
RbF	$Fm\bar{3}m$	PEM	RbF
RbF	$Pm\bar{3}m$	PEM	RbF
RbF	$Pm\bar{3}m$	PEM	RbF
ZnF_2	$P4_2/mnm$	PEM	ZnF_2
ZnF_2	$Pbcn$	PEM	ZnF_2
$NaZnF_3$	$Pnma$	ST	$(NaF)_{1.0}(ZnF_2)_{1.0}$
$NaZnF_3$	$Pbnm$	ST	$(NaF)_{1.0}(ZnF_2)_{1.0}$
$RbZnF_3$	$P6_3/mnc$	ST	$(RbF)_{1.0}(ZnF_2)_{1.0}$
K_2ZnF_4	$I4/mmm$	ST	$(KF)_{2.0}(ZnF_2)_{1.0}$
Liquid		SSM	$(KF)_{1.0}(ZnF_2)_{1.0}$

SSM: Subregular solution model; ST: stoichiometric compound; PEM: pure end-member.

$$x_A = |0.5 - \Delta x_A^{A,B,C}|, \tag{10}$$

$$x_B = (1 - x_A)x_B^{B,C} \tag{11}$$

and

$$x_B = (1 - x_A)x_C^{B,C} \tag{12}$$

where the T_A, $T_{fus}^{B,C}$, $x_B^{B,C}$, $x_C^{B,C}$, T_B and T_C has the same meaning as above. $\Delta x_A^{A,B,C}$, $\Delta x_A^{A,B}$ and $\Delta x_A^{A,C}$ can be calculated from the above Eqs. (7)–(9). Then, the corresponding components concentration can be obtained by the above mentioned calculated value. Table 5 lists the predicted components concentration for the ternary systems of the NaF-KF-RbF-ZnF_2 using this method.

2.3. Thermodynamic models

2.3.1. Lattice stabilities

As seen in Table 2, there are more than one crystal structures for RbF, ZnF_2 and $NaZnF_3$, of which more stable structures were employed in this work. For these pure end-members, their Gibbs energy functions can be expressed in the following equation [35],

$$^{o}G_i^{\phi}(T) = G_i^{\phi}(T) - H^{SER} = a + bT + cT\ln(T) + dT^2 + eT^3 + \frac{f}{T} + \sum_n g_n T^n \tag{13}$$

is the molar enthalpy of the stable element reference (SER) when the pure element is in its stable state at 298.15 K, T refers to the absolute temperature (K), a–f and g_n are coefficients, and n refers to the integers. All the coefficients appeared in Eq. (13) for the corresponding compounds are displayed in data in brief.

2.3.2. Thermodynamic modeling for liquid phase

The liquid phase was thermodynamically described by the classical subregular solution model, which has been successfully used to a series of molten salt systems [22–27]. The Gibbs energy equation of liquid is expressed in the Eq. (14).

$$G_{AF-BF}^{Liquid} = x_{AF}G_{AF}^{liq} + x_{BF}G_{B_F}^{liq} + RT(x_{AF}\ln x_{AF} + x_{BF}\ln x_{BF}) + x_{AF}x_{BF}^{\upsilon}L_{xAF,xBF}^{\mathrm{liq}}(x_{AF} - x_{BF})^{\upsilon} \tag{14}$$

Where x_{AF} and x_{BF} are the molar fraction of corresponding component AF and BF, and $\upsilon L_{x_{AF},x_{BF}}^{\mathrm{liq}}$ is the interaction parameter, which depends on temperature and is described as linear function $\upsilon L^{liq} = a_\upsilon + b_\upsilon T$.

2.3.3. Thermodynamic modeling for intermediate phases

There are five intermediate compounds $NaZnF_3$, $RbZnF_3$, Rb_2ZnF_4, K_2ZnF_4 and $KZnF_3$ in the NaF-KF-RbF-ZnF_2 quaternary system. They are thermodynamic described as the stoichiometric compounds model. Their Gibbs energy is expressed in the following Eq. (15).

$$G_{(AF)_x(BF)_y}^{solid} = xG_{AF}^{o} + yG_{BF}^{o} + \Delta_r H_{(AF)_x(BF)_y}^{o} - T\Delta_r S_{(AF)_x(BF)_y}^{o} \tag{15}$$

where G_{AF}^{o} and G_{BF}^{o} are Gibbs energy of pure species AF and BF. $\Delta_r H_{(AF)_x(BF)_y}^{o}$ and $\Delta_r S_{(AF)_x(BF)_y}^{o}$ are the enthalpy and entropy of formation of the intermediate compound $(AF)_x(BF)_y$, respectively. As described in the preceding Section 2.1, enthalpy of formation $\Delta_r H_{(AF)_x(BF)_y}^{o}$ of $NaZnF_3$, $RbZnF_3$, K_2ZnF_4 and $KZnF_3$ can be obtained from first-principle calculation, which is applied as the initial value of the subsequent optimization.

3. Results and discussion

The thermodynamic optimization was conducted in the Pan Optimizer module of PANDAT software using the weighted least squares approach. The formation enthalpies of $NaZnF_3$ (−14129.638 J/mol), $RbZnF_3$ (−40936.618 J/mol), K_2ZnF_4 (−25739.642 J/mol) and $KZnF_3$ (−27901.255 J/mol) from first-principles calculation were used as the initial value and introduced to optimize the corresponding thermodynamic parameters. The thermodynamic optimization was performed and repeated many times until an excellent agreement with experimental data was obtained within the allowable experimental

Table 3
Comparison with calculated values and key experimental points of all the binary systems (*: This work).

System	Reaction	Invariant point		References
		T/K	χ_{ZnF_2}	
NaF-ZnF_2	*Liquid* ↔ ZnF_2+$NaZnF_3$	949	0.668	[*]
		958	0.690	[17]
		983	0.660	[18]
	Liquid ↔ $NaZnF_3$	1021	0.500	[*]
		1021	0.500	[17]
		1028	0.500	[18]
	Liquid ↔ $NaZnF_3$+NaF	917	0.315	[*]
		908	0.330	[17]
		925	0.330	[18]
KF-ZnF_2	*Liquid* ↔ KF+K_2ZnF_4	947	0.200	[*]
		943 ± 10	0.210	[17]
	Liquid + $KZnF_3$ « K_2ZnF_4	992	0.272	[*]
		993	0.300	[17]
	Liquid ↔ $KZnF_3$	1123	0.500	[*]
		1123	0.500	[17]
	Liquid ↔ $KZnF_3$+ZnF_2	1012	0.734	[*]
		1013	0.800	[17]
RbF-ZnF_2	*Liquid* ↔ RbF+Rb_2ZnF_4	859	0.196	[*]
		868 ± 10	0.210	[17]
	Liquid + $RbZnF_3$ « Rb_2ZnF_4	900	0.292	[*]
		893	0.320	[17]
	Liquid ↔ $RbZnF_3$	996	0.500	[*]
		1003	0.500	[17]
	Liquid ↔ $RbZnF_3$+ZnF_2	923	0.694	[*]
		923	0.700	[17]
RbF-NaF		**T/K**	χ_{RbF}	
	Liquid ↔ NaF+RbF	941	0.673	[*]
		940	0.672	[12]
		948 ± 10	0.730	[17]
RbF-KF		**T/K**	χ_{RbF}	
	Liquid ↔ KF+RbF	1044	0.680	[*]
		1043	0.720	[19]

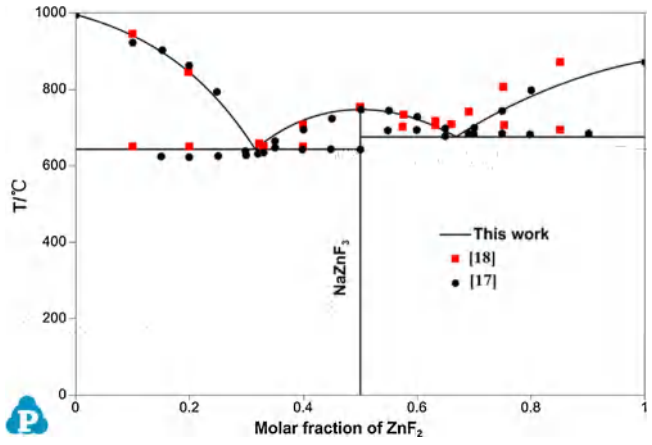

Fig. 1. Calculated phase diagram of NaF-ZnF_2 phase diagram.

errors limits. Phase diagrams were calculated and plotted using the PanPhaseDiagram module of PANDAT software, when the thermodynamic database for relative system was established. All model parameters optimized in the present work.

3.1. Binary systems

Based upon the thermodynamic databases of NaF-KF-RbF-ZnF_2 quaternary system, the calculated phase diagrams together with the experimental data for the relevant binary system have been plotted in the following section. Table 3 shows the comparison between the calculated value and key experimental data for all the binary systems from various resources.

The calculated phase diagram of NaF-ZnF_2 is displayed in Fig. 1 together with the experimental data form Thoma [17] and Kozak [18]. It is clearly manifested from Fig. 1 and Table 3 that the present calculated result is consistent with most of the experimental data, especially the congruently melting temperature of $NaZnF_3$, while somewhat deviates on the ZnF_2-rich side from Kozak [18]. Obviously, there is a large deviation between the melting point of ZnF_2 from Kozak [18] and the from Thoma [17] (This is the universally recognized melting point of ZnF_2 872 ℃). Thus, the optimized result is reliable and acceptable.

Figs. 2 and 3 show the phase diagram with the only reported

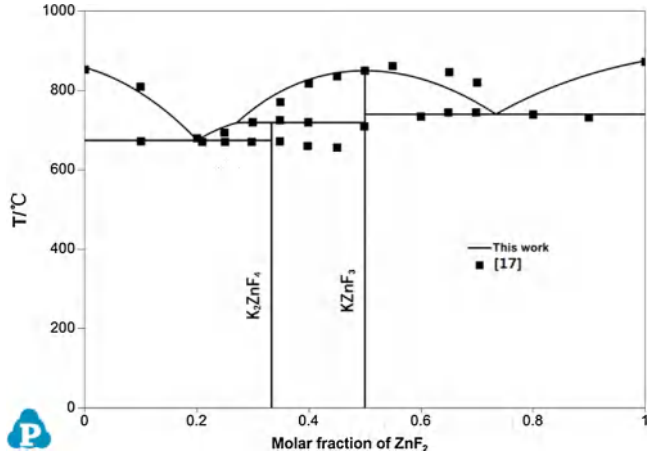

Fig. 2. Calculated phase diagram of KF-ZnF_2 phase diagram.

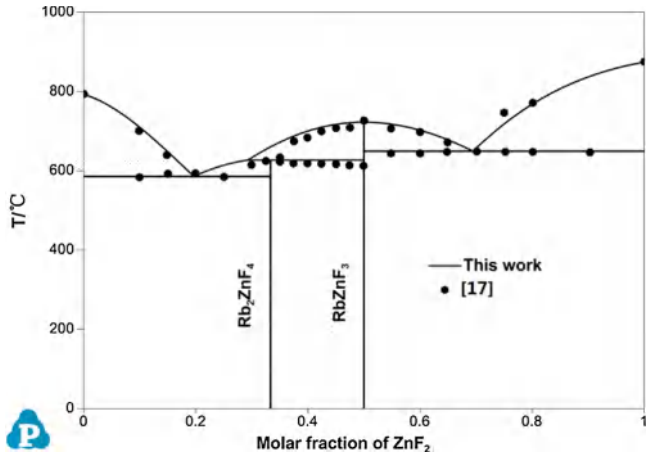

Fig. 3. Calculated phase diagram of RbF-ZnF_2 phase diagram.

Table 4
Comparison of formation enthalpy of intermediate phase between first-principles calculation and CALphad method.

Compound	$H_{\text{first- principles}}$ (kJ/mol)	H_{CALPhad} (kJ/mol)	Relative deviation $(\frac{H_{CALPhad}-H_{first-principles}}{H_{CALPhad}})$
$NaZnF_3$	−14129.638	−15040.100	6.05%
$KZnF_3$	−27901.255	−33048.400	15.57%
K_2ZnF_4	−25739.642	−36777.800	30.01%
$RbZnF_3$	−40936.618	−40570.300	-0.90%

experimental data from Thoma [17] for KF-ZnF_2 and RbF-ZnF_2 systems, respectively. The phase diagram of KF-ZnF_2 is observed to resemble that of the RbF-ZnF_2 with two intermediate phases. For KF-ZnF_2 system, it is evident from Fig. 2 and Table 3 that there is a good agreement between the calculated result and experimental data from Thoma [17], particularly the melting point of $KZnF_3$ (1123.75 K from calculated value compared with 1123.15 K from experimental measurement). Unfortunately, there exists a small deviation on the eutectic melting points composition between $KZnF_3$ and ZnF_2 (0.734 mol ZnF_2 from calculated value compared with 0.800 mol ZnF_2 from experimental measurement), while the calculated melting points temperature (1012.72 K) is in good accordance with the experimental data (1013.15 K). Compared with KF-ZnF_2 system, it can be observed from Fig. 3 and Table 4 that the optimized phase diagram of RbF-ZnF_2 can well and consistently reproduce all the experimental data.

The calculated RbF-NaF phase diagram is presented in Fig. 4 with the reported experimental data from Holm [12] and Thoma [17]. This is just a simple eutectic system without solid solution on both sides. It is evident from Fig. 4 and Table 3 that there is an excellent agreement between the calculated results and the relevant measured data.

Fig. 5 displays the calculated KF-RbF phase diagram in comparison with liquidus experimental data from Derfunov [19]. The calculated result can well reproduce the liquidus data and minimum temperature point observed from Fig. 5 and Table 3.

Comparisons of formation enthalpy of $NaZnF_3$, $KZnF_3$, K_2ZnF_4 and $RbZnF_3$ between first-principles calculation and CALphad method are listed in Table 4. As can be observed from Table 4, they are in good

Table 5
Calculated invariant points of the ternaries from the NaF-KF-RbF-ZnF_2 quaternary system (* and ※ refer to the value from phase diagram calculation and predicted value using the method in 2.2, respectively).

Ternary system (A-B-C)	Reaction type	Temp. (℃)	χ_A	χ_B	χ_C	resource
KF-NaF-RbF	$Liquid + Halite\#1 \xrightarrow{U} Solid + Halite\#2$	688.03	0.5698	0.3571	0.0731	[*]
KF-NaF-ZnF_2	$Liquid \xrightarrow{E1} K_2ZnF_4 + Halite\#2 + Halite\#1$	589.69	0.5259	0.2944	0.1797	[*]
			0.622	0.222	0.156	[※]
	$Liquid \xrightarrow{E2} K_2ZnF_4 + Halite\#2 + KZnF_3$	594.98	0.3888	0.3812	0.2300	[*]
	$Liquid \xrightarrow{E3} Halite\#2 + KZnF_3 + NaZnF_3$	593.90	0.1515	0.5512	0.2973	[*]
	$Liquid \xrightarrow{E4} KZnF_3+NaZnF_3+ZnF_2$	653.57	0.0852	0.2678	0.6470	[*]
KF-RbF-ZnF_2	$Liquid \xrightarrow{E1} Solid + K_2ZnF_4+RbZnF_3$	563.85	0.4056	0.3596	0.2348	[*]
	$Liquid \xrightarrow{E2} Solid + RbZnF_3+Rb_2ZnF_4$	565.43	0.3003	0.4744	0.2253	[*]
			0.263	0.560	0.177	[※]
	$Liquid \xrightarrow{E3} KZnF_3+RbZnF_3+ZnF_2$	636.86	0.0681	0.2571	0.6748	[*]
	$Liquid + KZnF_3 \xrightarrow{U} K_2ZnF_4+RbZnF_3$	584.48	0.4006	0.3391	0.2603	[*]
NaF-RbF-ZnF_2	$Liquid \xrightarrow{E1} NaF+RbZnF_3+NaZnF_3$	591.21	0.5300	0.1534	0.3166	[*]
	$Liquid \xrightarrow{E2} ZnF_2+RbZnF_3+NaZnF_3$	620.42	0.1616	0.1864	0.6520	[*]
	$Liquid \xrightarrow{E3} NaF+Rb_2ZnF_4+RbF$	549.74	0.1935	0.6478	0.1587	[*]
			0.130	0.699	0.171	[※]
	$Liquid + RbZnF_3 \xrightarrow{U} NaF+Rb_2ZnF_4$	579.27	0.2724	0.4883	0.2393	[*]

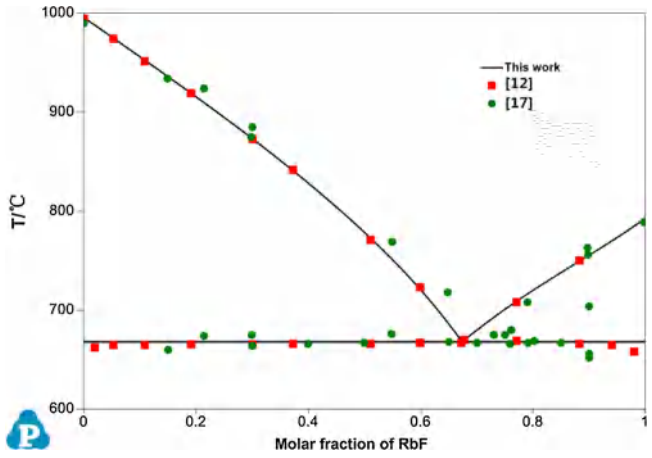

Fig. 4. Calculated phase diagram of NaF-RbF phase diagram.

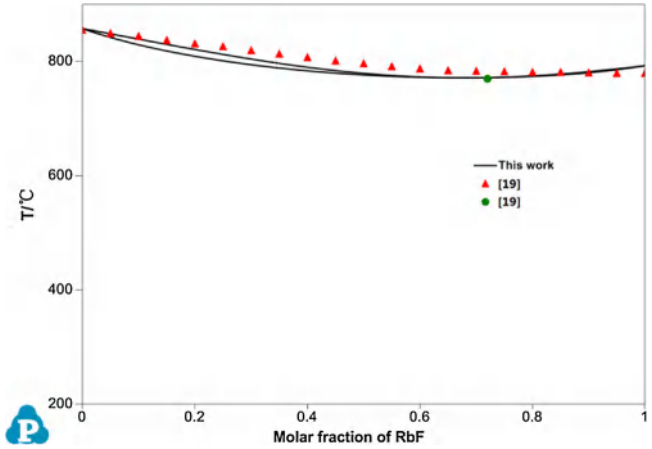

Fig. 5. Calculated phase diagram of KF-RbF phase diagram.

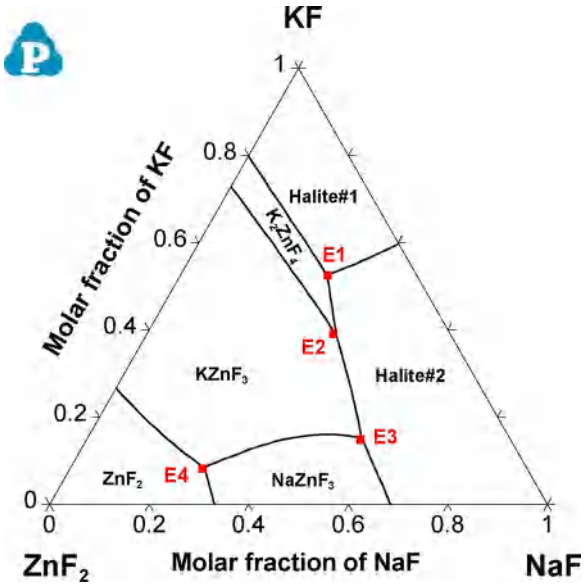

Fig. 6. The predicted liquidus projection of NaF-KF-ZnF_2 system.

correspondence with each other, except the formation enthalpy of K_2ZnF_4. Although there is a slight deviation for the formation enthalpy of K_2ZnF_4 from two different methods, the difference is reasonable and acceptable within the range of allowable errors, considering the first-principles calculation is performed at 0 K.

3.2. Ternary systems

According to thermodynamic database developed herein, a set of thermodynamic prediction on the thermodynamic properties of the sub-ternary systems have been conducted. Figs. 6–9 present the calculated liquidus projections of NaF-KF-ZnF_2, NaF-KF-RbF, NaF- RbF-ZnF_2 and KF- RbF-ZnF_2 systems with the primary phases. The calculated

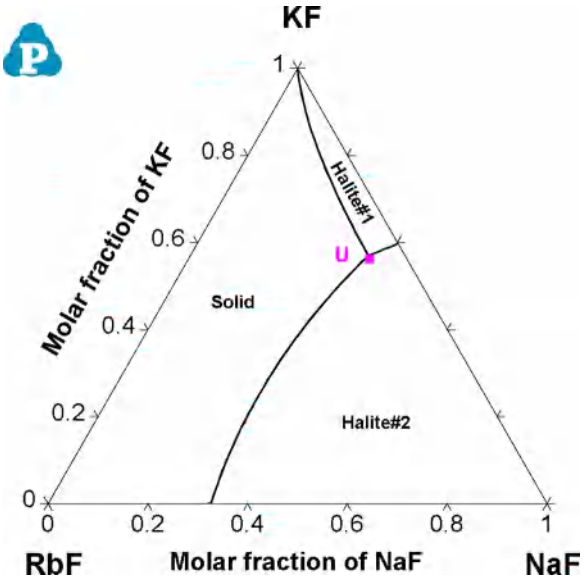

Fig. 7. The predicted liquidus projection of NaF-KF-RbF system.

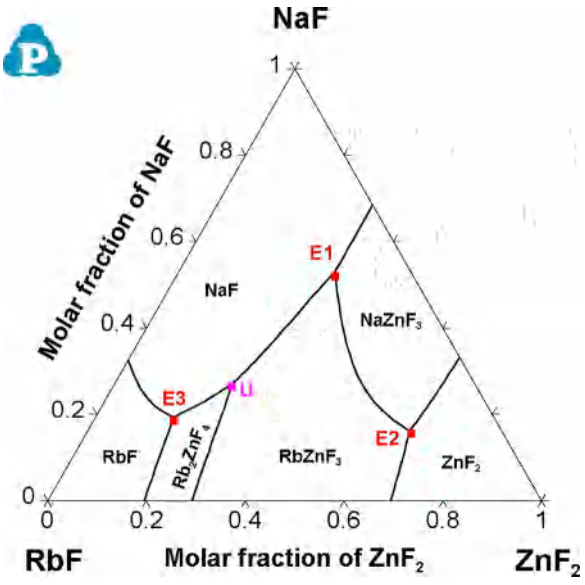

Fig. 8. The predicted liquidus projection of NaF- RbF-ZnF_2 system.

invariant reactions and temperature points of these ternary systems are displayed in Table 5, together with the predicted component concentration by the aforementioned method introduced in the 2.2. Here, the sign E and U in the Figs. 6–9 refer to the eutectic reaction ($L \xrightarrow{E} \alpha + \beta + \gamma$) and transition reaction ($L + \gamma \xrightarrow{U} \alpha + \beta$), respectively. The calculated value from phase diagram is reasonable connecting the predicted value of the aforementioned method in the 2.2, considering allowable experimental errors in this paper.

4. Conclusions

Thermodynamic optimizations have been conducted on the binary NaF-ZnF_2, KF-ZnF_2, RbF-ZnF_2, NaF-RbF and KF-RbF systems. The liquid phase was described by the subregular solution model, while the intermediate phases were treated as stoichiometric compounds. Model parameters were optimized on the basis of experimental phase equilibrium data and theoretical predictions from first-principles calculations. Comparisons of the calculation results with experimental data indicate that thermodynamic parameters of the five binary systems are

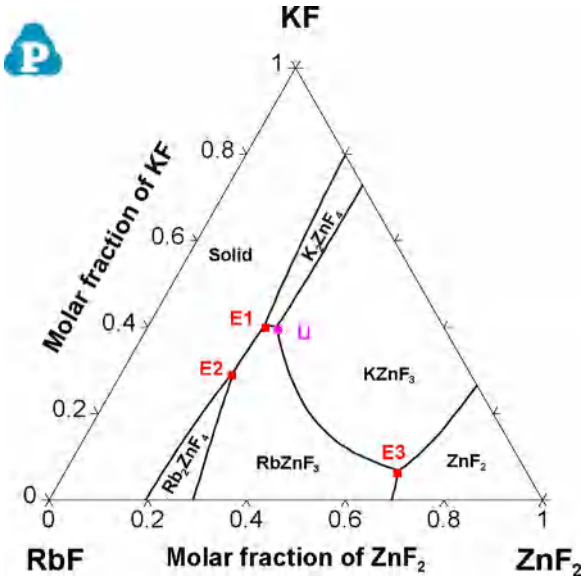

Fig. 9. The predicted liquidus projection of KF- RbF-ZnF_2 system.

reliable and acceptable in the present work. What's more, Furthermore, the thermodynamic properties and phase diagram for sub-ternary have been predicted, which are useful to provide the theoretical guide for the relative multi-components molten system design in the industrial application.

Acknowledgments

PANDANT Software from CompuTherm LLC is Gratefully Acknowledged. The authors deeply appreciate Wang Kun and Zhu Jun for the guidance of phase diagram optimization. This work is supported by Qinghai Major Science and Technology Projects (2017-GX-A3),National Natural Science Foundation of China (51601212, 51604257 and 21703281) and Transformational Technologies for Clean Energy and Demonstration (Grant No. XDA 21000000).

References

[1] D.E. Holcomb, S.M. Cetiner, An Overview of Liquid-Fluoride-Salt Heat Transport Systems, ORNL/TM-2010/156, USA, 2010.
[2] D.E. Holcomb, G.F. Flanagan, G.T. Mays, W.D. Pointer, K.R. Robb, G.L. Yoder, Fluoride Salt-Cooled High-Temperature Reactor Technology Development and Demonstration Roadmap, ORNL/TM-2013/401, USA, 2013.
[3] C. Forsberg, L.W. Hu, P. Peterson, K. Sridharan, Fluoride-Salt-Cooled High-Temperature Reactors (FHRs) for Power and Process Heat, MIT-ANP-TR-157, USA, 2014.
[4] M.W. Rosenthal, P.R. Kasten, R.B. Briggs, Nucl. Appl. Technol. 8 (1970) 107–117.
[5] D.F. Williams, Assessment of Candidate Molten Salt Coolants for the NGNP/NHI Heat-Transfer Loop, ORNL/TM-2006/69, USA, 2006.
[6] M. Mehos, C. Turchi, J. Vidal, M. Wagner, Z. Ma, C. Ho, W. Kolb, C. Andraka, A. Kruizenga, Concentrating Solar Power Gen3 Demonstration Roadmap, NREL/TP-5500-67464, USA, 2017.
[7] D.G. Lovering, An Introduction to Molten Salt Technology, Springer, Germany, 1982.
[8] G.J. Janz, J. Phys. Chem. Ref. Data 17 (1988) 1–325.
[9] A.G. Bergman, I.N. Nikonova, Zh. Obshch. Khim. 12 (1942) 449–459.
[10] A.G. Bergman, G.I. Nagornyi, Izv. Akad. Nauk SSSR Khim. (1943) 328–333.
[11] F.P. Platonov, Tr. Mosk S'kh Akad. 36 (1946) 42–44.
[12] J.L. Holm, L. Jan, A.L. Pikas, R. Ryhage, P.H. Nielsen, B. Sjöberg, E. Larsen, Acta Chem. Scand. 19 (1965) 638–644.
[13] A.C. Macleod, J. Cleland, J. Chem. Thermodyn. 7 (1975) 103–118.
[14] K.C. Hong, O.J. Kleppa, J. Chem. Thermodyn. 8 (1976) 31–36.
[15] S.J. Zhang, C. Brubaker, C. Jiang, M. Yang, Y. Zhong, Q.Y. Han, Z.K. Liu, Mater. Sci. Eng. A 418 (2006) 161–171.
[16] K. Wang, J.H. Cheng, P. Zhang, Y. Zuo, L.D. Xie, J. Univ. Sci. Technol. B. 36 (2017) 1666–1675.
[17] R.E. Thoma, ORNL report No. 2548, Oak Ridge, Tennessee, USA (1959).
[18] A.D. Kozak, M. Samouel, J. Less common Met. 40 (1975) 185–193.
[19] E.P. Dergunov, A.G. Bergman, Zh. Fiz. Khim. 22 (1948) 625–632.
[20] Y.A. Chang, S.L. Chen, F. Zhang, X.Y. Yan, F.Y. Xie, R. Schmid-Fetzer, W.A. Oates,

Prog. Mater. Sci. 49 (2004) 313–345.
[21] N. Saunders, A.P. Miodownik, CALPHAD (Calculation of Phase Diagrams): A Comprehensive Guide, Elsevier, Netherlands, 1998.
[22] X.H. An, P. Zhang, J.H. Cheng, S.L. Chen, J.Q. Wang, Chem. Res. Chin. Univ. 33 (2017) 122–128.
[23] X. Li, L.D. Xie, J. Alloys Compd. 736 (2018) 124–135.
[24] X. Li, S. Wu, Y. Wang, L.D. Xie, Appl. Energy 212 (2018) 516–526.
[25] H.Q. Yin, P. Zhang, X.H. An, J.H. Cheng, X. Li, S. Wu, X.J. Wu, W.G. Liu, L.D. Xie, J. Fluor. Chem. 209 (2018) 6–13.
[26] H.Q. Yin, K. Wang, L.D. Xie, H. Han, W.F. Wang, Chem. Res. Chin. Univ. 31 (2015) 461–465.
[27] S. Wu, X. Li, P. Zhang, X.H. An, L.D. Xie, Chem. Res. Chin. Univ. 34 (2018) 457–463.
[28] Z.K. Liu, J. Phase Equilib. Diff. 30 (2009) 517–534.
[29] G.Y. Sun, J. Kürti, P. Rajczy, M. Kertesz, J. Hafner, G. Kresse, J. Mol. Struct. 624 (2003) 37–45.
[30] J.P. Perdew, J.A. Chevary, S.H. Vosko, K.A. Jackson, M.R. Pederson, D.J. Singh, C. Fiolhais, Phys. Rev. B 46 (1992) 6671–6687.
[31] P.E. Blöchl, Phys. Rev. B 50 (1994) 17953–17979.
[32] M.P. Susarev, N.S. Martynova, J. Appl. Chem. USSR 47 (1974) 526–529.
[33] A.S. Trunin, O.E. Morgunova, M.V. Klimova, A.V. Budkin, Russ. J. Inorg. Chem. 51 (2006) 337–341.
[34] R. Rauda, R. Jacobb, F. Brunob, G. Willa, T.A. Steinberg, Renew. Sustain. Energy Rev. 70 (2017) 936–944.
[35] A.T. Dinsdale, Calphad 15 (1991) 317–425.